Mineral N stock and nitrate accumulation in the 50 to 200 m profile on the Loess Plateau

Xiaoxu Jia[a,b,c], Yuanjun Zhu[c,*], Laiming Huang[a,b,c], Xiaorong Wei[c], Yunting Fang[d], Lianhai Wu[e], Andrew Binley[f], Mingan Shao[a,b,c,*]

[a]Key Laboratory of Ecosystem Network Observation and Modeling, Institute of Geographic Sciences and Natural Resources Research, Chinese Academy of Sciences, Beijing, 100101, China;

[b]College of Resources and Environment, University of Chinese Academy of Sciences, Beijing, 100190, China;

[c]State Key Laboratory of Soil Erosion and Dryland Farming on the Loess Plateau, Northwest A&F University, Yangling Shaanxi, 712100, China;

[d]Key Laboratory of Forest Ecology and Management, Institute of Applied Ecology, Chinese Academy of Sciences, Shenyang, 110016, China;

[e]Rothamsted Research, North Wyke, Okehampton, Devon EX20 2SB, UK;

[f]Lancaster Environment Centre, Lancaster University, Bailrigg Lancaster, LA1 4YQ, UK

[*]Correspondence: Yuanjun Zhu (zhuyuanjun@foxmail.com) or Mingan Shao (shaoma@igsnrr.ac.cn), State Key Laboratory of Soil Erosion and Dryland Farming on the Loess Plateau, Northwest A&F University, Yangling Shaanxi, 712100, China.

Abstract: Nitrogen (N) stored in deep profiles is important in assessing regional and/or global N stocks and nitrate leaching risk to groundwater. The Chinese Loess Plateau, which is characterized by significantly thick loess deposits, potentially stores immense stocks of mineral N, posing future threats to groundwater quality. In order to determine the vertical distributions of nitrate and ammonium content in the region, as well as to characterize the potential accumulation of nitrate in the deep loess profile, we study loess samples collected at five sites (Yangling, Changwu, Fuxian, An'sai and Shenmu) through a 50 to 200 m loess profile. The estimated storage of mineral N varied significantly among the five sites, ranging from 0.46 to 2.43 × 10^4 kg N ha^{-1}. Ammonium exhibited fluctuations and dominated mineral N stocks within the whole profile at the sites, except for the upper 20-30 m at Yangling and Changwu. Measured nitrate content in the entire profile at Fuxian, An'sai and Shenmu is low, but significant accumulations were observed to 30-50 m depth at the other two sites. Analysis of $\delta^{15}N$ and $\delta^{18}O$ of nitrate indicates different causes for accumulated nitrate at these two sites. Mineralization and nitrification of manure and organic N respectively contribute nitrate to the 0-12 and 12-30 m profile at Changwu; while nitrification of NH_4^+ fertilizer, NO_3^- fertilizer and nitrification of organic N control the nitrate distribution in the 0-3, 3-7 and 7-10 m layer at Yangling, respectively. Furthermore, our analysis illustrates the low denitrification potential in the lower part of the vadose zone. The accumulated nitrate introduced by human activities is thus mainly distributed in the upper vadose zone (above 30 m), indicating, currently, a low nitrate leaching risk to groundwater due to a high storage capacity of the thick vadose

zone in the region.

Key words: Nitrate; Ammonium; Nitrate accumulation; Critical Zone; The Loess Plateau

1. Introduction

Over use of synthetic nitrogen (N) fertilizer (and/or manure) as well as increased deposition of atmospheric N have adversely and chronically affected soil and water quality, human health, biodiversity and ecosystem functions around the world (Vitousek et al., 1997, 2009; Galloway et al., 2003; Walvoord et al., 2003; Zhu et al., 2005; Guo et al., 2010). To understand and manage the environmental impacts of mineral nitrogen, N reservoirs, sources and cycling rates have been studied at a wide range of scales to quantify N budgets (Cleveland et al., 1999; Galloway et al., 2003; Jin et al., 2015; Quan et al., 2016). Investigations of soil N within the upper 1 m soil depth, defined operationally as the biologically active soil zone or the root zone in most agricultural systems, where N turnover is rapid (Schlesinger et al., 1990), as well as lower vadose zone beyond the root zone, have been conducted around the world (Mercado, 1976; Walvoord et al., 2003; Izbicki et al., 2015; Turkeltaub et al., 2015; Huang et al., 2016). However, the scarcity of measured deep N data still limits the regional and/or global estimation of N stock, especially for some regions with thick sedimentary deposits. For example, consideration of desert subsoil N storage could raise estimates of vadose zone N inventory by 14 to 71% for warm deserts and arid shrublands worldwide and by 3 to 16% globally (Walvoord et al., 2003). In a recent study, Ascott et al. (2017) estimate 605-1814 Tg of nitrate stored in pore waters in the vadose zone across the globe.

Soil N is immobilized by microbes or fixed by clay minerals, but also exists as nitrate (NO_3-N) or ammonium (NH_4-N) in the soil matrix (Sebilo et al., 2013). Because nitrate is very dynamic and mobile (Gu et al., 2013), subsoil nitrate can leach beyond the reach of roots, eventually leaching to groundwater, causing nitrate contamination and consequently a threat to human health (Babiker et al., 2004). Moreover, nitrate accumulated in the topsoil layer is considered to have very different environmental impacts compared to that leached to the subsoil layer (Zhou et al., 2016). Therefore, quantifying the magnitude and distribution characteristics of subsoil N can provide additional information on understanding of N cycling within thick soil profiles, which will help improving residual N management and assessing the nitrate leaching risk.

The Loess Plateau (LP) is located in the middle reach of the Yellow River in North China and is the deepest and largest loess deposit in the world (Yang et al., 1988). Parts of the region, e.g., the Guanzhong Plain and some tableland areas, have experienced intensive agricultural activities for hundreds of years (Wei et al., 2010). A number of investigations on the plateau have been conducted to investigate the distribution patterns of soil nitrate and ammonium in the profiles and study the loss and accumulation of nitrate in the root zone, which have shown that long-term application of N fertilizer or manure as well as increased nitrate deposition resulting from the rapid development of petroleum and coal industries in this region can significantly increase residual N in the soil and pose a potential threat to groundwater (Lü et al., 1998; Fan et al., 2010; Wei et al., 2010; Jin et al., 2015). However, most of these studies have focused on the top 4 m soil layer. Several studies measured N at depths deeper than 4 m, but usually less than 20 m (Jin et al., 2015; Zhou et al., 2016). Leakage of nitrate may occur below such depth, gradually moving downward to the deeper vadose zone and to groundwater (Zhou et al., 2016; Huang et al., 2018). Furthermore, the LP is predominantly covered by loessial deposits, which range in thickness from 30 to 200 m (Zhu et al., 2018). This deep deposit means that the LP has high potential for storing nitrogen or other nutrients. Therefore, there is a need for N data to facilitate evaluations of the stock of mineral N and in order to understand N cycles that occur in the deep profiles in the LP. Further research is also needed to determine the depth and extent of leached nitrate, particularly given the environmental sensitivity of the LP region.

We hypothesize that (1) there may be a significant nitrate accumulation in the deep vadose zone, particularly in the southern parts of the region which experience much higher precipitation and more intensive agricultural activities and (2) accumulated nitrate in the deep vadose zone cannot be denitrified due to lack of dissolved organic carbon. To address these hypotheses, loess samples from the land surface to bedrock (approximately 50-200 m) at five sites from the south to the north of the plateau were analyzed to determine nitrate and ammonium concentrations. The specific objectives of this study were (1) to investigate the distribution characteristics of mineral N (NO_3-N and NH_4-N) between the surface and bedrock on the LP, (2) to assess the size of mineral N stock within thick loess deposits, and (3) to characterize the potential nitrate accumulation in the deeper vadose zone by analyzing natural abundance of nitrate N and O isotopes.

2. Materials and methods

2.1. Study area

This study was conducted on the Chinese LP (33.72 -41.27°N, 100.90 -114.55°E and 200-3000 m a.s.l., Fig. 1) that covers a total area of 640,000 km^2. The region has a continental monsoon climate with the mean annual precipitation (MAP) ranging from 150 mm in the northwest to 800 mm in the southeast, most (55-78%) of which falls in June through September. The mean annual temperature (MAT) is 3.6°C in the northwest and increases to 14.3°C in the southeast (1953-2013 data from 64 weather stations). The thickness of loess deposits ranges from 30 to 200 m, with an average of 92.2 m (Zhu et al., 2018), and sandy in texture in the northwest and more clayey in the southeast. The LP topography is characterized by Yuan (a large flat surface with little or no erosion), Liang (a long narrow range of hills), Mao (an oval-to-round loess hill) and gullies of all shapes and forms (Yang et al., 1988). The plateau can be divided into three sub-regions according to water availability to ecosystems: the Mu Us Desert in the driest northwest sector of the plateau; an area of irrigated agriculture within the main stem of the Yellow River catchment in the southeast plateau; and the rain-fed hilly area in the middle of the plateau (Fig. 1).

2.2. Borehole drilling and sediment sample collection

Five boreholes were drilled along a south-north direction on the LP: Yangling (YL), Changwu (CW), Fuxian (FX), An'sai (AS) and Shenmu (SM) (Fig. 1). A single borehole (15 cm in diameter) at each site was drilled from the land surface to bedrock between May and June 2016 using the under-reamer method, also known as the ODEX (Overburden Drilling EXploration) air-hammer drilling method (Izbicki et al., 2000). The drilling depth ranged from 56 to 205 m. A description of each site is shown in Table 1. The croplands at sites FX, AS and SM have been abandoned for natural vegetation restoration since 2000 to control soil erosion.

Entire loess cores were collected at 1 m intervals from the land surface to bedrock at each site. At YL, sediment samples were collected at 0.5 m intervals in the top 10 m depth in order to consider the effect of intensive human activities, and then at 1 m intervals below that. A total of 728 loess cores were collected in 1 m long PVC core-barrel liners. Subsamples consisting of 2 kg of loess were collected from the center of each core and sealed in plastic sampling bags. All the subsamples were encased in ice boxes for transport on the same day to the laboratory and stored in 4°C refrigerators until analysis. These subsamples were analyzed for the particle size distribution, bulk density, pH, NO_3-N and NH_4-N and ^{15}N and ^{18}O in nitrate.

2.3. Analyses of loess physicochemical properties and isotope

The particle size distribution was determined by laser-diffraction (Mastersizer 2000, Malvern Instruments, Malvern, England) (Fig. S1). Bulk density was measured using a soil bulk sampler with a 5.0 cm diameter by 5.0 cm height stainless steel cutting ring for each core by measuring the dry mass after oven-drying at 105°C for 48 hrs. Loess pH was measured using a pH meter with a loess-to-water ratio of 1:2.5. The loess samples were extracted with 2 M potassium chloride (KCl) solution in their moist state (soil:solution, 1:5) and then filtered through a 0.45-μm filter. The KCl extract was analyzed immediately for NH_4-N and NO_3-N concentrations using a Lachat Flow Injection Analyzer (AutoAnalyzer3-AA3, Seal Analytical, Mequon, WI) (Kachurina et al., 2000). In order to identify the sources of accumulated nitrate, the isotope compositions of nitrate ($\delta^{15}N$ and $\delta^{18}O$) were analyzed based on the isotopic analysis of the produced N_2O from NO_3-N (Liu et al., 2017). The value is expressed as:

$$\delta(‰) = \left(\frac{R_{sample}}{R_{standard}} - 1\right) \times 1000 \qquad (1)$$

where R denotes the ratio of the heavy isotope to the light isotope for N or O. The isotopic signatures of the produced N_2O were determined by an IsoPrime 100 continuous flow isotope ratio mass spectrometer connected to a trace gas (TG) preconcentrator (Liu et al., 2014).

Stocks of nitrate or ammonium (S_i, quantity of N per unit area, kg N ha^{-1}) in a loess core were calculated by the concentration (C_{on}), bulk density (BD) and the length of the core (L):

$$S_i = Con_i \times BD \times L \qquad (2)$$

where i is nitrate or ammonium.

2.4. Statistical analysis

Statistically significant differences in the concentrations and stocks of nitrate and ammonium among the five boreholes were identified using a one-way analysis of variance (ANOVA) followed by a least significant difference (LSD) test ($P < 0.05$). All statistical analyses were performed with the Statistical Program for Social Sciences (SPSS 16.0; SPSS Inc., Chicago, IL, USA).

3. Results

3.1. Particle size distribution and pH among the five boreholes

Mean percentages of sand, silt and clay in the whole profile exhibited significant differences between FX, AS and SM but not between YL and CW. However, clay content was significantly lower and sand content higher at FX, AS and SM compared with those at YL and CW. Relatively higher clay and silt contents were found at FX, whereas the highest sand content and lowest silt content at SM (Table 2 and Fig. S1). The averaged pH of the whole profile at CW and AS was the highest, followed by SM and the lowest at YL and FX (Table 2).

3.2. Mineral N contents and stock

The contents of loess NO_3-N and NH_4-N from surface to bedrock for the five boreholes are presented in Fig. 2. NO_3-N content in the 0-5 m loess profile at YL and CW shows a progressive depletion pattern and then significant accumulation at the depth of 5-55 and 5-30 m, respectively. Below these depths, concentrations remain low and display minimal variation. The average measured NO_3-N content over 0-55 m (YL) and 0-30 m (CW) is about 14 (YL) and 9 (CW) times higher than that at lower depth. At the other three sites (FX, AS and SM) the measured NO_3-N content is low and shows little variation throughout the profile. Samples from YL and CW have significantly higher content in the 0-30 m profile than the other three boreholes (Fig. 3). In the 30-60 m profile, the measured content is not significantly different among CW, FX, AS and SM, but significantly higher at YL. Whereas below 60 m, no difference in NO_3-N content among the sites was observed.

Measured NH_4-N content exhibits fluctuations within profiles for the five boreholes (Fig. 2). The average content through the entire profile at FX is the highest (7.43 mg N kg^{-1}), followed by SM (5.11 mg N kg^{-1}). No significant differences were detected among the other three boreholes (Fig. S2). NH_4-N is the dominant form of mineral N preserved in the entire profile at FX, AS and SM, and the ratios of NO_3-N/NH_4-N averaged 0.10, 0.10 and 0.05, respectively (Fig. 4). In the upper 20 m of the profile at YL, the content was much lower or comparable to NO_3-N content, and the ratio of NO_3-N/NH_4-N averaged 1.23. A similar result was observed in the upper 30 m of the profile at CW, and the ratio of NO_3-N/NH_4-N averaged 1.21, whereas below 30 m, NH_4-N was the dominant form of mineral N.

The total mineral N stored in the entire profile is 2.43, 1.27, 0.46, 1.04 and 1.87 $\times 10^4$ kg N ha^{-1} at FX, AS, SM, YL and CW, respectively (Fig. 5). However, NH_4-N in the entire profile represented approximately 92, 92 and 97% of total mineral N at FX, AS and SM, respectively, but 71 and 78% at YL and CW, respectively. The vertical distribution of NO_3-N followed its content distribution at each site (Fig. S3). NO_3-N was 0.28 and 0.24 × 10^4 kg N ha^{-1} in the upper 55 and 30 m of the profile and approximately 45 and 54% of the amount of the total mineral N at YL and CW, respectively.

3.3. Nitrogen and oxygen isotopes in nitrate

As shown in Fig. 6, the measured isotopic composition of nitrate in the upper 10 m of the profile at YL varies from -1.50 to +6.52‰ for $\delta^{15}N$ and from -5.46 to +24.68‰ for $\delta^{18}O$, with a mean of +2.60 and +9.34‰, respectively. The values of $\delta^{15}N$ and $\delta^{18}O$ in the upper 30 m of the profile at CW vary from +4.33 to +17.47‰ and -14.24 to +0.08‰, respectively. The mean $\delta^{15}N$ and $\delta^{18}O$ values in the top 30 m of the profile at CW are +8.51 and -6.03‰, respectively.

4. Discussion

The depth of the five boreholes showed spatial variations in the thickness of loess deposit on the Chinese LP. The shallowest of the loess profile was found in the north of the plateau with approximately 60 m and deepest in the south of the plateau with 205 m. We analyzed particle size distribution, bulk density, pH, NO_3-N and NH_4-N contents and ^{15}N and ^{18}O in nitrate at 1 m intervals. This is the first time loess samples have been taken to such depths on the plateau and also first step to investigate nutrient cycling in the critical zone of the LP.

Mineral N stock in the entire loess profiles also showed spatial variation, which is primarily caused by variations in the loess depth and NH_4-N and NO_3-N contents. FX has the largest stock of mineral N because of its highest NH_4-N content and thick loess deposit (190 m). A larger stock of mineral N at CW than that at the other three boreholes can be attributed to its thickest loess deposit (205 m) and a higher NO_3-N content in the upper 30 m layer. Although the depth of loess at YL was 57 m lower than that at AS, the amount of mineral N at YL is comparable to that at AS, which could be ascribed to the higher NO_3-N content in the upper 55 m layer. Assuming that comparable inventories (0.46 to 2.43 × 10^4 kg ha^{-1}) exist in the 4.3 × 10^7 ha of typical loess region on the plateau (Fig. 1), there might be approximately 0.2 to 1.0 Pg mineral N stored in the loess profile in the region, indicating a large mineral N reservoir in the LP. This compares to global total estimates of 95 Pg in the top meter of soils (Post et al., 1985).

The NO_3-N content in the 0-5 m soil profile at YL and CW decreased with depth and show significant nutrient depletion patterns (Fig. 2), which could be attributed to root uptake and a shorter life cycle of nitrate. A similar pattern was observed in the 0-2 m soil profile at FX. It is reported that the roots of dominant crops (winter wheat and maize) in the study area can reach 3.2 m or even deeper (Li, 1983), which can consume soil water and nutrients in the deep soil profile. In contrast, ammonium content showed little changes with soil depth and remained at a low and stable level around 3.0 and 4.0 mg N kg^{-1} in the 0-5 m soil profile at YL and CW, respectively. This result may be related to volatilization. Previous studies have found that

NH_4^+-formed fertilizer or urea, a dominant type of fertilizer applied to calcareous soils with pH > 8.0, are easily volatilized in the semi-arid and semi-humid regions in China (Zhang et al., 1992; Wang et al., 2014). Furthermore, the ratio of NO_3-N to NH_4-N remained constant in the profile from surface to bedrock at the five sites except for the upper 50 m layer at YL and upper 30 m layer at CW, within which significant nitrate accumulation was found (Fig. 4). This result suggests that nitrate accumulation in the deep loess profile altered the initial relationship between nitrate and ammonium and thus the N budgets. Nevertheless, the baseline level of NH_4-N in the entire loess profile was much higher than NO_3-N in the LP region, indicating that NH_4-N is the dominant form of mineral N preserved in the profile, agreed with Jin et al. (2015). The level of loess NH_4-N is nearly four to twenty times higher than that of NO_3-N (Fig. 2). Low temperature in the deep loess profile can inhibit the ammonium oxidation rate (Delgado-Baquerizo et al., 2013; Zhang et al., 2013; Wang et al., 2014), which is beneficial to the loess ammonium storage (Hu et al., 2008). Furthermore, because of the positive charge of ammonium, opposite to clay in most cases, the residual ammonium is fixed by clay minerals or immobilized by organic matter (Zhou et al., 2016). We infer that ammonium, resulting from wet and dry deposition, may have been preserved in the deep profile during the loess deposition over millions of years. The magnitude of ammonium within different loess layers may be related to environmental conditions over a geological period. While there is few strong evidence to explain why there is a higher ammonium than nitrate in the deep loess profile in the present study, further research needs to be performed to study this interesting issue.

Compared to the NO_3-N content at FX, AS and SM, there is a significant accumulation in the upper 50 m at YL and 30 m at CW, and occurs far beyond the crop root zone, which supports our hypothesis that there is a significant nitrate accumulation in a deeper vadose zone, particularly in the southern parts of the region. Similar observations were also reported in arid and semi-arid desert sites in the western United States, where the highest concentrations were between 20 and 40 m below land surface (Izbicki et al., 2015). Although both YL and CW are located in intensive agricultural areas, more nitrate is accumulated in the loess profile and transported deeper at YL than that at CW. Numerous studies have suggested that soil texture (Tong et al., 2005; Fan et al., 2010), hydrology (Stonestrom et al., 2003; Gates et al., 2008; Ju et al., 2009; Hartmann, 2014), fertilizer application (Zhang et al., 2004; Ju et al., 2006; Zhou et al., 2016) and crop systems (Fan et al., 2010; Turkeltaub et al., 2015; Zhou et al., 2016) could significantly affect NO_3-N accumulation in the profile. There are three possible reasons for the higher NO_3-N accumulation at YL than CW. Firstly, a greater amount of N fertilizer is applied because of the use of double cropping systems and the much longer agricultural history at YL (Fan et al., 2010); secondly, more nitrate leaches because of relatively high precipitation coupled with irrigation at YL; and thirdly, a higher atmospheric NO_3-N deposition rate at YL (Liang et al., 2014). In contrast to YL and CW, there is no significant NO_3-N accumulation in the loess profile at the other three sites, which could be ascribed to low precipitation and a lower N fertilizer application rate along with land use change. In the north part of the plateau, the arid and semi-arid region, the application rate of N fertilizer or manure is much lower than in the south of the plateau due to low productivity limited by low water supply (Zhou et al., 2016). Rainwater infiltration is mostly limited to the 0-1 m soil layer in both normal and wet years in the region because of high evapotranspiration and low precipitation (Liu and Shao, 2016; Jia et al., 2017a), limiting nitrate transport to deeper layers. Moreover, from 1999, farmers have been converting their cropland into natural grassland, shrubland or forestland to control soil erosion (Jia et al., 2017a, b), which could significantly alter recharge processes and consequently nitrate transport (Kurtzman and Scanlon, 2011). Grasses and shrubs can take up more soil mineral N and water because of their longer growing periods and deeper roots than crops (Jia et al., 2017b, c), hindering NO_3-N flow from shallow soil to deep soil layers (Fan et al., 2005; Huang et al., 2018).

The isotope analysis suggests different sources for accumulated nitrate at YL and CW (Fig. 6). In the irrigated agricultural region where YL is located, nitrate in the top 3 m of soil is mostly likely derived from NH_4^+-formed fertilizer through nitrification, while that in the 3-7 and 7-10 m layer is contributed by NO_3^--formed fertilizer and organic N via mineralization and nitrification, respectively. This result indicates that nitrate derived from NH_4^+-formed fertilizer remained in the upper 0-3 m soil layer, while nitrate derived from NO_3^--formed fertilizer had transported to the lower vadose zone with water flow. This conclusion corresponds to the current agricultural management practices in the area: intense fertilizer application (NH_4^+-NO_3^- fertilizer or urea for summer maize and winter wheat) and subsequent irrigation. In the rain-fed agricultural region, CW, however, manure and organic N might be significant contributors to nitrate in the 0-12 and 12-30 m layer, respectively, as the $\delta^{15}N\text{-}NO_3^-$ values range from +4.3‰ to 17.5‰. This result reflects single source of nitrate in the upper 0-12 m layer in CW. During the recent 60 years at CW, manure has been the most important source of N applied to farmland soils with an average application rate of 24.9 ton ha^{-1} (Wei et al., 2010). However, $\delta^{15}N$ ranges are overlapped for some N sources, such as domestic and animal effluents, making it difficult to identify specific sources. Complementary tracers, such as, the boron isotope ratio ($\delta^{11}B$) should be considered to better segregate different nitrate sources, especially for soil NH_4^+, manure or septic waste (Briand et al., 2016). The different texture of the profiles can cause different patterns of $\delta^{15}N$ even when only one kind of fertilizer is applied (Zhang et al., 2013). A relatively coarse texture may favor nitrate transport to move down to the deeper vadose zone. Texture of the profiles in both YL and CW, however, is very similar and uniform in the upper 0-50 m profile (Fig. S1); the effects of texture on nitrate transport can thus be ignored. The different sources of nitrate between YL and CW were caused by different agricultural activities. Fertilizer applied in YL was $NH_4^+\text{-}NO_3^-$ fertilizer or urea, while manure was applied in CW. Furthermore, the changes in sources of nitrate within different layers appeared as sequential migration across the profile. This may be related to the water flow mechanisms (piston flow or preferential flow) and application of different fertilizers during different periods. We infer that water flow in the deep vadose zone is in the form of piston flow due to the relatively uniform and dense texture of the profiles in the southern LP (Zhang et al., 2013; Huang et al., 2018). Nevertheless, isotopic composition of nitrate ($\delta^{15}N$ and

$\delta^{18}O$) in sediment samples clearly support a low leaching process and mobilization of solutes across the vadose zone in the LP due to limited recharge. Recharge rate rather than solute concentration controls deep vadose zone and groundwater quality in the arid and semiarid LP region (Radford et al., 2009; Huang et al., 2018). Furthermore, revegetation in the study area may decrease the recharge rate and consequently the nitrate leaching process (Huang et al., 2018).

Denitrification can make residual nitrate enriched in ^{15}N and the $\delta^{15}N$ value of residual nitrate increases with decreasing nitrate content (Mariotti et al., 1981). It has been reported that the ratio of $\delta^{15}N/\delta^{18}O$ ranges from 1.3 to 2.1 (Böttcher et al., 1990; Liu et al., 2006). In our study, there was no significantly negative correlation between $\delta^{15}N$ and nitrate content (data not shown) and the $\delta^{15}N$ and $\delta^{18}O$ values do not strongly follow the denitrification slope at both YL and CW (Fig. 6), which indicates that the denitrification potential is very low in the deep vadose zone. This result supports the second hypothesis that accumulated nitrate in the deeper vadose zone cannot be denitrified and is consistent with previous studies (Zhang et al., 2013; Yuan, 2015; Zhou et al., 2016). In the arid and semi-arid regions, nitrate can be preserved with limited denitrification (Edmunds and Gaye, 1997; Hartsough et al., 2001) because of prevalent aerobic conditions (Winograd and Robrtson, 1982) and absence of organic matter (Edmunds, 2009). Therefore, accumulated nitrate can exist for decades or even hundreds of years and gradually move downward to the deeper vadose zone with water flow, which may finally reach groundwater.

Nitrate brought in by human activities at both YL and CW, however, has not entered the aquifer because of the thick vadose zone (Fig. 2). This suggests that the storage capacity of the vadose zone can delay nitrate into the aquifer (Mercado, 1976; Izbicki et al., 2015; Huang et al., 2016), allowing time for developing and implementing policies to address future water-quality issues. Continuous N fertilization may not cause nitrate contamination to groundwater in the areas with a deep groundwater level on the plateau in a short term but would leach to groundwater rapidly in the area with shallow vadose zone or groundwater table on the plateau (Emteryd et al., 1998; Fan et al., 2010). Therefore, different agricultural management practices should be considered in agricultural areas with a different vadose zone thickness on the plateau. Management alternatives should also be further investigated to help curb nitrate concentration increase in the vadose zone.

5. Conclusions

Through analysis of loess nitrogen in five deep cores taken from the Loess Plateau we have provided more insight into nitrogen stocks and dominant processes controlling such stocks. Ammonium was the dominant form of mineral N preserved in the profile from surface to bedrock at the five sites except for the upper 20 m layer at YL and 30 m layer at CW, within which significant nitrate accumulation was found. Nitrate in the entire loess profile, however, remains at a low and stable level at FX, AS and SM. Nevertheless, we have revealed a potentially large reservoir of mineral N within the plateau. Nitrate may have accumulated in the upper 50 m layer in the irrigated agricultural area, represented by YL, in the southern edge of the plateau, which has experienced long-term and intensive agricultural activities; while in the rain-fed agricultural area, e.g., CW, south central of the plateau, nitrate may have accumulated at shallow depths (30 m in the loess profile analyzed here). Nitrogen and oxygen isotope analysis indicates that the most important source of nitrate is from NH_4^+ fertilizer through nitrification in the upper 3 m soil, but this is supplemented by NO_3^- fertilizer and organic N via nitrification in the 3-10 m layer at YL; whilst at CW the main sources are from manure and organic N through nitrification in the upper 30 m of the profile. Nitrate accumulation beyond the root zone, can exist for a long term in the Loess Plateau because of limited nitrate denitrification due to the presence of oxygen and lack of carbon sources. Our results highlight the need for more attention to be paid to understanding the pattern of nitrate throughout the vadose zone and an assessment of the nitrate leaching risk to groundwater.

Acknowledgements

This research was supported by the National Natural Science Foundation of China (41571130081), the NERC Newton Fund through the China-UK collaborative research on critical zone science (NE/N007433/1 and NE/N007409/1), the Youth Innovation Promotion Association of the Chinese Academy of Sciences (2017076) and the Youth Innovation Research Team Project (LENOM2016Q0001). We acknowledge the help of J.B Qiao and J Wang in collecting sediment samples. We are also grateful to G.Q Ren, L.L Song and Y Tu for their kind help in analysis of isotope compositions of nitrate.

References

Ascott, M., Gooddy, D.C., Wang, L., Stuart, M.E., Lewis, M.A., Ward, R.S., Binley, A.M. 2017. Global Patterns of Nitrate Storage in the Vadose Zone. Nat. Commun. 8(1), doi:10.1038/s41467-017-01321-w.

Babiker, I.S., Mohamed, M.A.A., Terao, H., Kato, K., Ohta, K., 2004. Assessment of groundwater contamination by nitrate leaching from intensive vegetable cultivation using geographical information system. Environ. Int. 29, 1009-1017.

Briand, C., Sebilo, M., Louvat, P., Chesnot, T., Vaury, V., Schneider, M., Plagnes, V., 2016. Legacy of contaminant N sources to the NO3- signature in rivers: a combined isotopic (δ^{15}N-NO_3-, δ^{18}O-NO_3-, δ^{11}B) and microbiological investigation. Sci. Rep. 7, 10.1038/srep41703.

Böttcher, J., Strebel, O., Voerkelius, S., Schmidt, H.L., 1990. Using isotope fractionation of nitrate-nitrogen and nitrate-oxygen for evaluation of microbial denitrification in a sandy aquifer. J. Hydrol. 114, 413-424.

Cleveland, C.C., Townsend, A.R., Schimel, D.S., Fisher, H., Howarth, R.W., Hedin, L.O., Perakis, S.S., Latty, E.F., Von Fischer, J.C., Elseroad, A., 1999. Global patterns of terrestrial biological nitrogen (N-2) fixation in natural ecosystems. Global Biogeochem. Cy. 13, 623-645.

Delgado-Baquerizo, M., Maestre, F.T., Gallardo, A., Bowker, M.A., Wallenstein, M.D., et al. 2013. Decoupling of soil nutrient cycles as a function of aridity in global drylands. Nature 502, 672-676.

Edmunds, W.M., Gaye, C.B., 1997. Naturally high nitrate concentrations in groundwaters from the Sahel. J Environ. Qual. 26, 1231-1239.

Edmunds, W.M., 2009. Geochemistry's vital contribution to solving water resource problems.

Appl. Geochem. 24, 1058-1073.

Emteryd, O., Lu, D.Q., Nykvist, N., 1998. Nitrate in soil profiles and nitrate pollution of drinking water in the Loess Region of China. Ambio 27, 441-443.

Fan, J., Shao, M.A., Hao, M.D., Wang, Q.J., 2005. Nitrate accumulation and distribution in soil profiles in ecosystem of upland on the Loess Plateau. Plant Nutr. Fert. Sci. 11, 8-12. (in Chinese)

Fan, J., Hao, M.D., Malhi, S.S., 2010. Accumulation of nitrate-N in the soil profile and its implications for the environment under dryland agriculture in northern China: A review. Can. J. Soil Sci. 90, 429-440.

Galloway, J.N., Aber, J.D., Erisman, J.W., Seitzinger, S.P., Howarth, R.W., Cowling, E.B., Cosby, B.J., 2003. The nitrogen cascade. Bioscience 53, 341-356.

Gates, J.B., Böhlke, J.K., Edmunds, W.M., 2008. Ecohydrological factors affecting nitrate concentrations in a phreatic desert aquifer in northwestern China. Environ. Sci. Technol. 42, 3531-3537.

Gu, B.J., Ge, Y., Chang, S.X., Luo, W., Chang, J., 2013. Nitrate in groundwater of China: Sources and driving forces. Global Environ. Change 23, 1112-1121.

Guo, J.H., Liu, X.J., Zhang, Y., Shen, J.L., Han, W.X., Zhang, W.F., Christie, P., Goulding, K.W.T., Vitousek, P.M., Zhang, F.S., 2010. Significant acidification in major Chinese croplands. Science 327, 1008-1010.

Hartmann, T.E., 2014. Nitrogen dynamics, apparent mineralization and balance calculations in a maize-wheat double cropping system of the North China Plain. Field. Crop. Res. 160, 22-30.

Hartsough, P., Tyler, S.W., Sterling, J., Walvoord, M., 2001. A 14.6 kyr record of nitrogen flux from desert soil profiles as inferred from vadose zone pore waters. Geophys. Res. Lett. 28, 2955-2958.

Huang, T.M., Yang, S., Liu, J., Li, Z., 2016. How much information can soil solute profiles reveal about groundwater recharge? Geosci. J. 20, 495-502.

Huang, Y.N., Chang, Q.R., Li, Z., 2018. Land use change impacts on the amount and quality of recharge water in the loess tablelands of China. Sci. Total Environ. 628-629, 443-452.

Hu, L., Lee, X.Q., Huang, D.K., Cheng, J.Z., 2008. Ammonium nitrogen in surface soil of arid and semiarid Central East Asia. Geochemica 37, 572-580.

Izbicki, J.A., Radyk, J., Michel, R.L., 2000. Water movement through a thick unsaturated zone underlying an international stream in the western Mojave Desert, southern California, USA. J Hydrol. 238, 194-217.

Izbicki, J.A., Flint, A.L., O'Leary, D.R., Nishikawa, T., Martin, P., Johnson, R.D., Clark, D.A., 2015. Storage and mobilization of natural and septic nitrate in thick unsaturated zones, California. J Hydrol. 524, 147-165.

Jia, X.X., Wang, Y.Q., Shao, M.A., Luo, Y., Zhang, C.C., 2017a. Estimating regional losses of soil water due to the conversion of agricultural land to forest in China's Loess Plateau. Ecohydrology 10, 10.1002/eco.1851.

Jia, X.X., Shao, M.A., Zhu, Y.J., Luo, Y., 2017b. Soil moisture decline due to afforestation across the Loess Plateau, China. J Hydrol. 546, 113-122.

Jia, X.X., Yang, Y., Zhang, C.C., Shao, M.A., Huang, L.M., 2017c. A state-space analysis of soil organic carbon in China's Loess Plateau. Land Degrad. Develop. 28, 983-993.

Jin, Z., Zhu, Y.J., Li, X.R., Dong, Y.S., An, Z.S., 2015. Soil N retention and nitrate leaching in three types of dunes in the Mu Us desert of China. Sci. Rep. 5, 10.1038/srep14222.

Jobbágy, E.G., Jackson, R.B., 2001. The distribution of soil nutrients with depth: Global patterns and the imprint of plants. Biogeochemistry 53, 51-77.

Ju, X.T., Kou, C.L., Zhang, F.S., Christie, P., 2006. Nitrogen balance and groundwater nitrate contamination: Comparison among three intensive cropping systems on the North China Plain. Environ. Pollut. 143, 117-125.

Ju, X.T., Xing, G.X., Chen, X.P., Zhang, S.L., Zhang, L.J., Liu, X.J., Cui, Z.L., Yin, B., Christie, P., Zhu, Z.L., Zhang, F.S., 2009. Reducing environmental risk by improving N management in intensive Chinese agricultural systems. Proc. Natl. Acad. Sci. USA 106, 3041-3046.

Kachurina, O.M., Zhang, H., Raun, W.R., Krenzer, E.G., 2000. Simultaneous determination of soil aluminum, ammonium- and nitrate-nitrogen using 1 M potassium chloride extraction. Commun. Soil Sci. Plan. 31, 893-903.

Kurtzman, D., Scanlon, B.R., 2011. Groundwater Recharge through Vertisols: Irrigated Cropland vs. Natural Land, Israel. Vadose Zone J. 10, 662-674.

Li, Y.S., 1983. The properties of water cycle in soil and their effect on water cycle for land in the Loess Plateau. Acta Ecol. Sin. 3, 91-101 (in Chinese).

Liang, T., Tong, Y.A., Lin, W., Qiao, L., Liu, X.J., Bai, S.C., Yang, X.L., 2014. Spatial-temporal variability of dry and wet deposition of atmospheric nitrogen in different ecological regions of Shaanxi. Acta Ecol. Sin. 34,738-745. (in Chinese)

Liu, B.X., Shao, M.A., 2016. Response of soil water dynamics to precipitation years under different vegetation types on the northern Loess Plateau, China. J Arid Land 8, 47-59.

Liu, D.W., Zhu, W.X., Wang, X.B., Pan, Y.P., Wang, C., Xi, D., Bai, E., Wang, Y.S., Han, X.G., Fang, Y.T., 2017. Abiotic versus biotic controls on soil nitrogen cycling in drylands along a 3200 km transect. Biogeosciences 14, 989-1001.

Liu, D.W., Fang, Y.T., Tu, Y., Pan, Y.P., 2014. Chemical method for nitrogen isotopic analysis of ammonium at natural abundance. Anal. Chem. 86, 3787-3792.

Liu, C.Q., Li, S.L., Lang, Y.C., Xiao, H.Y., 2006. Using δ^{15}N- and δ^{18}O-values to identify nitrate sources in Karst ground water, Guiyang, Southwest China. Environ. Sci. Technol. 40, 6928-6933.

Lü, D.Q., Tong, Y.A., Sun, B.H., 1998. Study on effect of nitrogen fertilizer use on environment pollution. Plant Nutr. Fert. Sci. 4, 8-15. (in Chinese)

Mariotti, A., Germon, J.C., Hubert, P., Kaiser, P., Letolle, R., Tardieux, A., Tardieux, P., 1981. Experimental determination of nitrogen kinetic isotope fractionation: some principles; illustration for the denitrification and nitrification processes. Plant Soil 62, 413-430.

Mercado, A., 1976. Nitrate and chloride pollution of aquifers: A regional study with the aid of a single-cell model. Water Resour. Res. 12(4), 731-747.

Post, W.M., Pastor, J., Zinke, P.J., Stangenberger, A.G., 1985. Global patterns of soil nitrogen storage. Nature 317, 613-616.

Quan, Z., Huang, B., Lu, C.Y., Shi, Y., Chen, X., Zhang, H.Y., Fang, Y.T., 2016. The fate of fertilizer nitrogen in a high nitrate accumulated agricultural soil. Sci. Rep. 6, 10.1038/srep21539.

Radford, B.J., Silburn, D.M., Forster, B.A., 2009. Soil chloride and deep drainage responses to land clearing for cropping at seven sites in central Queensland, northern Australia. J Hydrol. 379, 20-29.

Schlesinger, W.H., Reynolds, J.F., Cunningham, G.L., Huenneke, L.F., Jarrell, W.M., Virginia, R.A., Whitford, W.G., 1990. Biological feedbacks in global desertification. Science 247, 1043-1048.

Sebilo, M., Mayer, B., Nicolardot, B., Pinay, G., Mariotti, A., 2013. Long-term fate of nitrate fertilizer in agricultural soils. Proc. Natl. Acad. Sci. USA 110, 18185-18189.

Stonestrom, D.A., Prudic, D.E., Laczniak, R.J., Akstin, K.C., Boyd, R.A., Henkelman, K.K., 2003. Estimates of deep percolation beneath native vegetation, irrigated Fields, and the Amargosa River channel, Amargosa Desert, Nye County, Nevada. Open-File Report — U.S. Geol. Surv. 03-104.

Tong, Y.A., Shi, W., Lu, D.Q., Emteryd, O., 2005. Relationship between soil texture and nitrate distribution and accumulation in three types of soil profile in Shaanxi. Plant Nutr. Fert. Sci. 11, 435-441. (in Chinese)

Turkeltaub, T., Kurtzman, D., Russak, E.E., Dahan, O., 2015. Impact of switching crop type on water and solute fluxes in deep vadose zone. Water Resour. Res. 51, 9828-9842.

Vitousek, P.M., Aber, J.D., Howarth, R.W., Likens, G.E., Matson, P.A., Schindler, D.W., Schlesinger, W.H., Tilman, D., 1997. Human alteration of the global nitrogen cycle: Sources and consequences. Ecol. Appl. 7, 737-750.

Vitousek, P.M., Naylor, R., Crews, T., David, M.B., Drinkwater, L.E., Holland, E., Johnes, P.J., Katzenberger, J., Martinelli, L.A., Matson, P.A., Nziguheba, G., Ojima, D., Palm, C.A., Robertson, G.P., Sanchez, P.A., Townsend, A.R., Zhang, F.S., 2009. Nutrient imbalances in agricultural development. Nature 324, 1519-1520.

Walvoord, M.A., Phillips, F.M., Stonestrom, D.A., Evans, R.D., Hartsough, P.C., Newman, B.D., Striegl, R.G., 2003. A reservoir of nitrate beneath desert soils. Science 302, 1021-2014.

Wang, C., Wang, X.B., Liu, D.W., Wu, H.H., Lü, X.T., Fang, Y.T., Cheng, W.X., Luo, W.T., Jiang, P., Shi, J., Yin, H.Q., Zhou, J.Z., Han, X.G., Bai, E., 2014. Aridity threshold in controlling ecosystem nitrogen cycling in arid and semi-arid grasslands. Nat. Commun. 5, 10.1038/ncomms5799.

Wei, X.R., Hao, M.D., Xue, X.H., Shi, P., Robert, H., Wang, A., Zhang, Y.F., 2010. Nitrous oxide emission from highland winter wheat field after long-term fertilization. Biogeosciences 7, 3301-3310.

Winograd, I.J., Robertson, F.N., 1982. Deep oxygenated groundwater: anomaly or common occurrence? Science 216, 1227-1230.

Yang, Q.Y., Zhang, B.P., Zheng, D., 1988. On the boundary of the Loess Plateau. J. Nat. Resour. 3, 9-15 (in Chinese).

Yuan, H.J., 2015. Denitrification in the deep soil from intensive farmlands in the North China Plain, Center for Agricultural Resources Research, Institute of Genetics and Development Biology, CAS.

Zhang, C.Y., Zhang, S., Yin, M.Y., Ma, L.N., He, Z., Ning, Z., 2013. Nitrogen isotope studies of nitrate contamination of the thick vadose zones in the wastewater-irrigated area. Environ. Earth Sci. 68, 1475-1483.

Zhang, J.B., Cai, Z.C., Zhu, T.B., Yang, W.Y., Muller, C., 2013. Mechanisms for the retention of inorganic N in acidic forest soils of southern China. Sci. Rep. 3, 10.1038/srep02342.

Zhang, S.X., Li, X.Y., Li, X.P., Yuan, F.M., Yao, Z.H., Sun, Y.L., Zhang, F.D., 2004. Crop yield, N uptake and nitrates in a fluvo-aquic soil profile. Pedosphere 14, 131-136.

Zhang, S.L., Cai, G.X., Wang, X.Z., Xu, Y.H., Zhu, Z.L., Freney, J.R., 1992. Losses of urea-nitrogen applied to maize on a calcareous fluvo-aquic soil in North China Plain. Pedosphere 2, 171-178.

Zhou, J.Y., Gu, B.J., Schlesinger, W.H., Ju, X.T., 2016. Significant accumulation of nitrate in Chinese semi-humid croplands. Sci. Rep. 6, 10.1038/srep25088.

Zhu, A.N., Zhang, J.B., Zhao, B.Z., Cheng, Z.H., Li, L.P., 2005. Water balance and nitrate leaching losses under intensive crop production with Ochric Aquic Cambosols in North China Plain. Environ. Int. 31, 904-912.

Zhu, Y.J., Jia, X.X., Shao, M.A., 2018. Loess thickness variations across the Loess Plateau of China. Surv. Geophys. doi: 10.1007/s10712-018-9462-6.

Figure captions:

Figure 1. Distribution of the Chinese Loess Plateau and locations of the five study sites. Maps were created using ArcGIS software by Esri (Environmental Systems Resource Institute, ArcGIS 10.0; www.esri.com).

Figure 2. Vertical distribution of NO_3-N and NH_4-N from the ground surface to bedrock at the borehole sites.

Figure 3. Differences in NO_3-N content among five boreholes at the depths of 0-30, 30-60 and > 60 m. In each boxplot, the *lower boundary* of the box shows the 25th percentile and the *upper boundary* shows the 75th percentile. The *crosses* extend from the boxes to the highest and lowest values, and the *lines* across the boxes indicate the median. The means of boxplots with *different lowercase letters* differ significantly at the 0.05 significance level (LSD test). YL, CW, FX, AS and SM refer to Yangling, Changwu, Fuxian, An'sai and Shenmu, respectively.

Figure 4. Vertical distribution of mineral N (NO_3-N + NH_4-N) storage at 1-m interval and ratio of NO_3-N to NH_4-N at YL, CW, FX, AS and SM sites.

Figure 5. Storage of NO_3-N, NH_4-N and total mineral N in an entire profile at Yangling (YL), Changwu (CW), Fuxian (FX), An'sai (AS) and Shenmu (SM) sites.

Figure 6. Cross-plot of ^{15}N-NO_3^- versus ^{18}O-NO_3^- in loess profile at Yangling (YL) and Changwu (CW). The typical ranges of the different nitrate end-members and the two typical trends (1.3:1 and 2.1:1) for denitrification in the diagram are modified after Liu et al.[44]

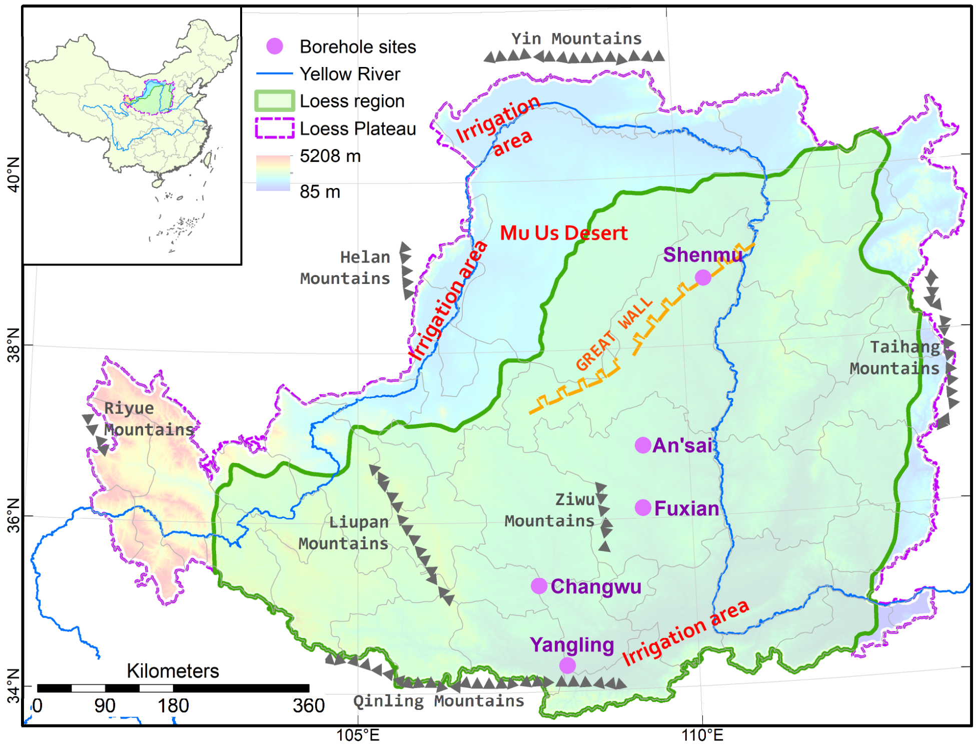

Figure 1. Distribution of the Chinese Loess Plateau and locations of the five study sites. Maps were created using ArcGIS software by Esri (Environmental Systems Resource Institute, ArcGIS 10.0; www.esri.com).

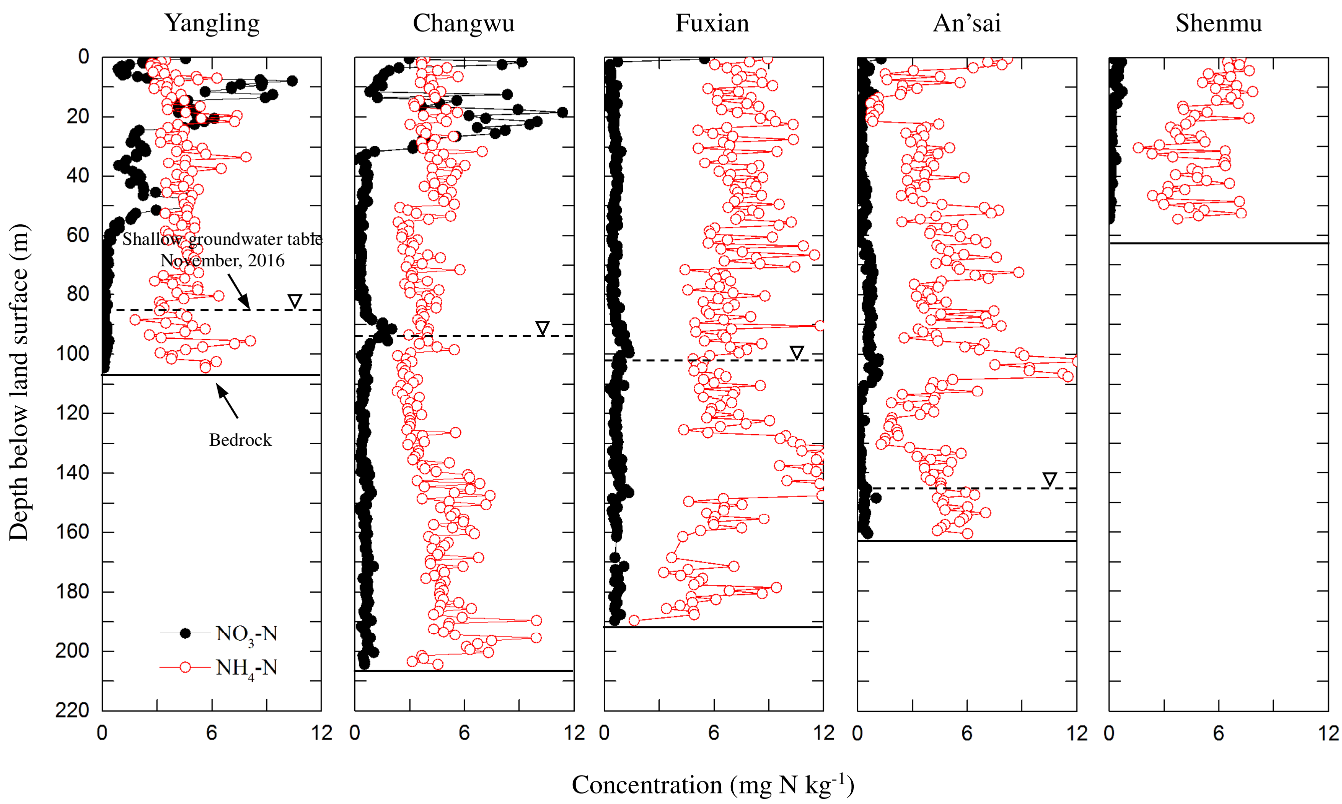

Figure 2. Vertical distribution of NO_3-N and NH_4-N from the ground surface to bedrock at the borehole sites.

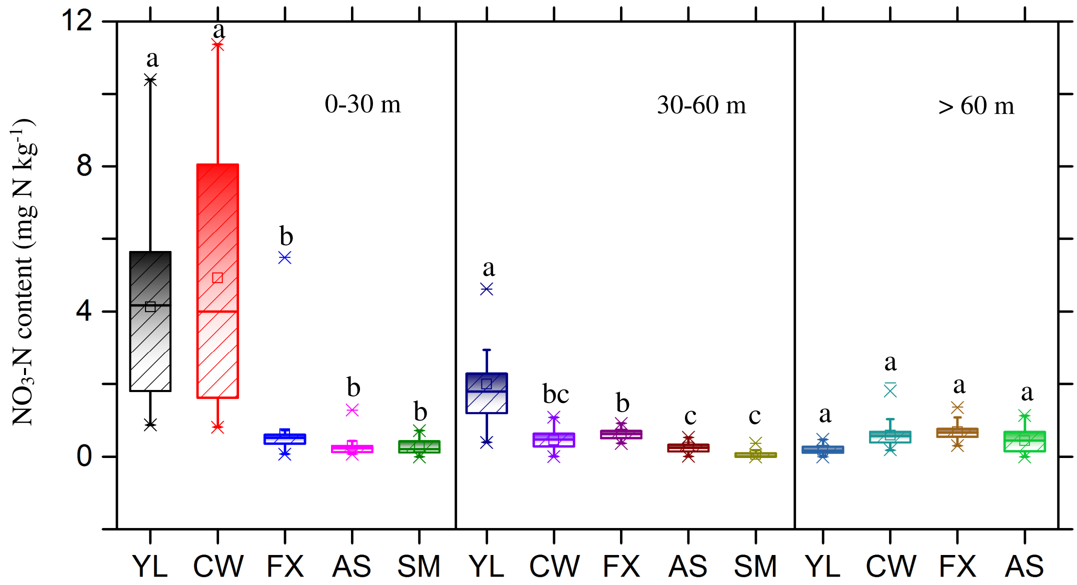

Figure 3. Differences in NO_3-N content among five boreholes at the depths of 0-30, 30-60 and > 60 m. In each boxplot, the *lower boundary* of the box shows the 25th percentile and the *upper boundary* shows the 75th percentile. The *crosses* extend from the boxes to the highest and lowest values, and the *lines* across the boxes indicate the median. The means of boxplots with *different lowercase letters* differ significantly at the 0.05 significance level (LSD test). YL, CW, FX, AS and SM refer to Yangling, Changwu, Fuxian, An'sai and Shenmu, respectively.

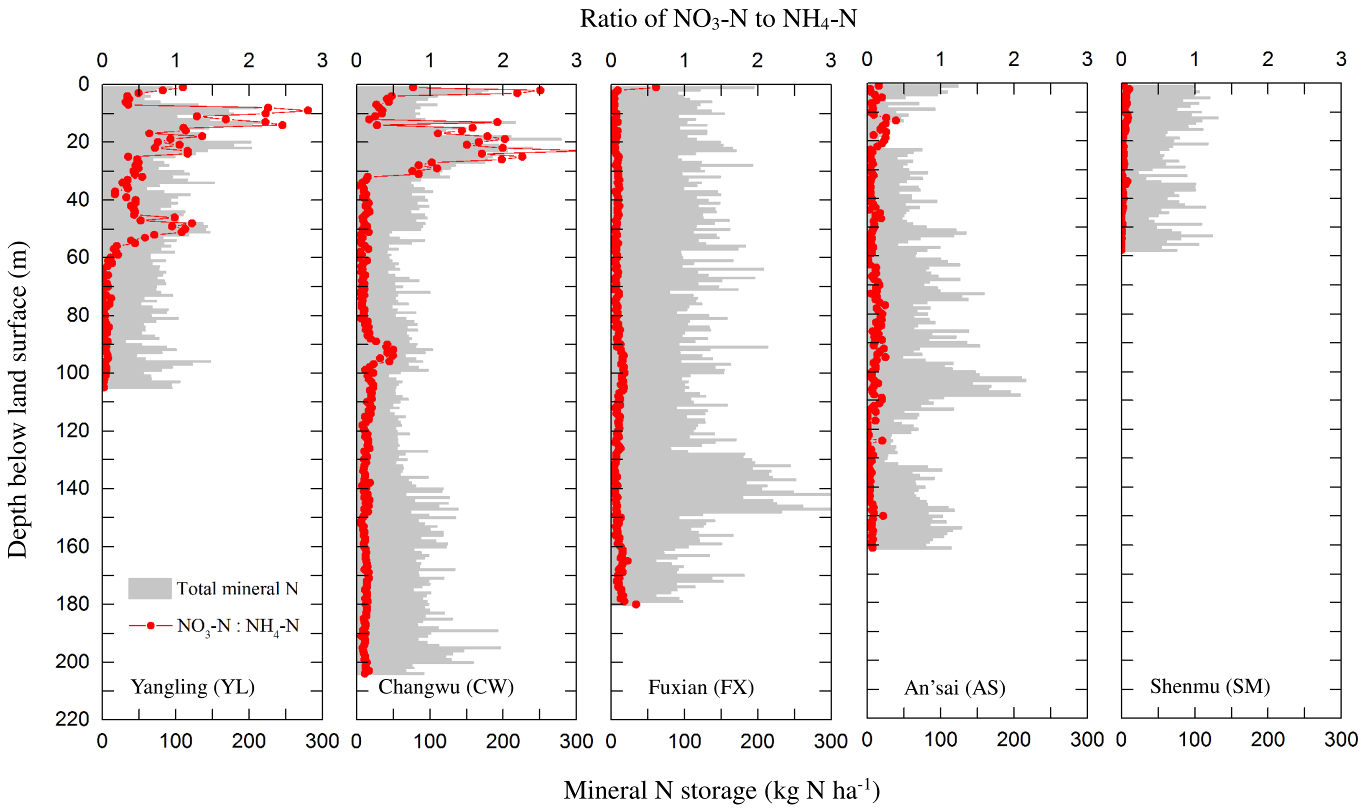

Figure 4. Vertical distribution of mineral N (NO_3-N + NH_4-N) storage at 1-m interval and ratio of NO_3-N to NH_4-N at YL, CW, FX, AS and SM sites.

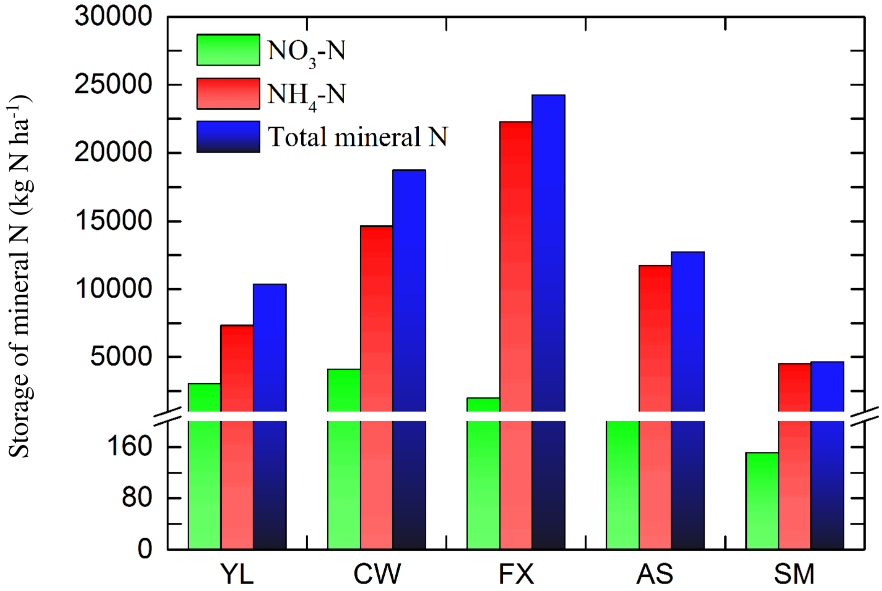

Figure 5. Storage of NO_3-N, NH_4-N and total mineral N in an entire profile at Yangling (YL), Changwu (CW), Fuxian (FX), An'sai (AS) and Shenmu (SM) sites.

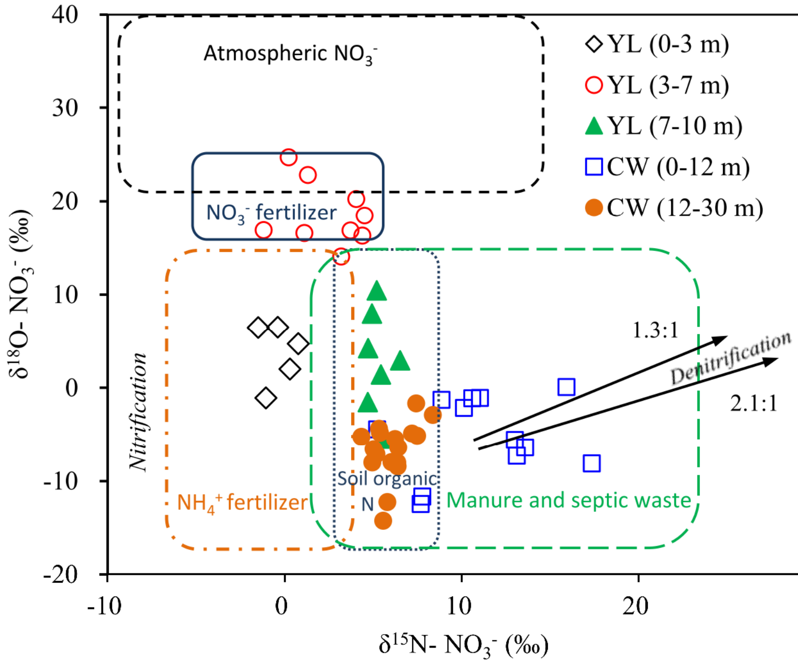

Figure 6. Cross-plot of ^{15}N-NO_3^- versus ^{18}O-NO_3^- in loess profile at Yangling (YL) and Changwu (CW). The typical ranges of the different nitrate end-members and the two typical trends (1.3:1 and 2.1:1) for denitrification in the diagram are modified after Liu et al.[44]